

# Investigation of High-Frequency Fine Structure in the Current Output of Shaped Contact Planar Gunn Diodes

A. Mindil , G. M. Dunn, A. Khalid , and C. H. Oxley

**Abstract**— *A novel gallium arsenide (GaAs) planar Gunn diode design with shaped anode and cathode contacts using Monte Carlo simulations has been shown to produce significantly higher frequency fine structure components in the output waveform than the natural transit time frequency of the diode. We have investigated devices without a feed- back potential and devices with a feedback potential (in the delayed mode) and have shown 350-GHz fine structure frequency components in a device with a nominal transit time frequency of 70 GHz is possible. This is the first observation of such stable repeating high-frequency components in a Gunn diode, giving potential for very high-frequency power generation and other wave-shaping applications.*

**Index Terms**— *Gallium arsenide (GaAs), high frequency, Monte Carlo, multiple peaks, planar Gunn diode.*

## I. INTRODUCTION

GUNN diodes, also known as a transferred electron devices (TEDs), are commonly used as a solid-state source of stable low-noise microwave radiation [1]. In the past few years, there has been continued research to increase operating frequency, efficiency, and output power for both vertical and planar Gunn diodes [2]–[5]. While over the years, most research has focused on vertical Gunn structures, and in the last decade, there has been an interest in the planar Gunn diode structure [2].

Manuscript received January 20, 2020; revised March 4, 2020; accepted March 12, 2020. Date of publication April 8, 2020; date of current version April 22, 2020. This work was supported by the Ministry of Higher Education of Saudi Arabia. The review of this article was arranged by Editor G. Ghione. (*Corresponding author: A. Mindil.*)

A. Mindil and G. M. Dunn are with the Department of Physics, School of Natural and Computing Sciences, University of Aberdeen, Aberdeen AB24 3UE, U.K. (e-mail: r01amhm@abdn.ac.uk; g.m.dunn@abdn.ac.uk).

A. Khalid is with the Centre of Electronic Warfare, Information and Cyber, Cranfield University, Defence Academy of the United Kingdom, Shrivenham SN6 8LA, U.K. (e-mail: ata.khalid@cranfield.ac.uk).

C. H. Oxley was with the School of Engineering and Sustainable Development, De Montfort University, Leicester LE1 9BH, U.K. He is now with De Montfort University, Leicester LE1 9BH, U.K.

The planar Gunn diode offers significant advantages when compared to the vertical Gunn diode. It can be more easily integrated into microwave monolithic integrated circuit (MMIC) technology, and the natural fundamental frequency of operation of the device is determined by the spacing between the anode and cathode contacts known as the channel length. This spacing is determined by fabrication, which offers more control than that by material growth process as required for the vertical Gunn diode. Planar Gunn devices have been demonstrated to operate at high frequencies, for example, an  $\text{In}_{0.53}\text{Ga}_{0.47}\text{As}$  planar Gunn diode gave a fundamental frequency of over 300 GHz for a  $0.6\text{-}\mu\text{m}$  channel length [3] and operating frequencies into the THz region may be possible in some material systems [6]. However, the output power and efficiency of these devices have remained low [7], preventing the diode from reaching its full commercial potential. The reasons for the low output power have been investigated by the authors, and work has shown uneven heating in the channel [8] inferring uneven current distribution [8] particularly at the channel edges. It was found that edge effects at the channel impair the development of Gunn domains and indeed observations of electroluminescence at the sharp corners of the channel [9] suggest the existence of high electric fields. Attempts to reduce the high electric fields that cause impact ionization at the anode-contact electrode have been investigated by novel contact design [10]. Monte Carlo simulations of the channel edge have indeed shown the importance of the shape of the anode and cathode corners on domain formation, and the simulations showed that sharp corners can lead to poorly formed and distorted domains. It was found that this could be corrected by shaping the contact corners to reduce the strength of the field [11].

Planar Gunn diodes offer the possibility of exploring other novel contact shaping, which differs from the morphology of the default linear parallel design of the cathode and anode. Very small feature sizes are possible, thus allowing intricate designs to be investigated, and the technology to achieve this will be discussed in Section III-D. Circular geometries were explored in [12], while investigations into different sizes of anode and cathode in a vertical Gunn geometry have been published in [13]. Simulations of a crenelated cathode in [14] showed the curious effect on the shape of the domain of this nonparallel design.

The natural fundamental frequency of a planar Gunn diode is determined by the width of the channel and the velocity of the domain. As the channel region width becomes shorter, there is less room for the domain to form and meeting the well-known  $\omega l$  (channel doping channel width) product rule [15], which limits the frequency of operation of a Gunn diode. Fabricating devices smaller than one micrometer is difficult, as the electron densities for good operation need to be high and such devices suffer from undesirable heating effects in the channel region.

To overcome this limitation, one idea that presents itself is for a single Gunn domain to be incident on a shaped anode giving a graded channel width; thus, the domain hits this contact multiple times, causing an increase in current each time. The current output of such a device would no longer be solely dependent on the period of time of transit but would have frequency components dependent on the separation of the points of contact between the cathode and shaped anode, which might possibly be considerably shorter than the width of the channel.

However, in a normal planar Gunn with a perfectly straight anode, the shape of the sharp corner at the edge of the channel can have an important effect on the shape of the Gunn domain as discussed earlier. Introducing a more complicated shaping of the anode may cause chaotic dynamics within the device with the domain forming and reforming in ever more complicated shapes on each subsequent transit. In [16], a shaped cathode was shown to produce a very complicated current waveform, probably from the aforementioned chaotic dynamics, and when analyzed was found to contain many frequency components.

In this article, using an ensemble Monte Carlo (EMC) method, we will demonstrate a planar Gunn diode design that produces stable, repeating domains, yielding a simple current waveform with multiple peaks corresponding to each transit of the domain. This was achieved using a simple applied dc potential without feedback and a delayed mode transit with feedback [17], [18].

## II. DEVICE DESIGN AND SIMULATION

An EMC method was used to simulate the carrier transport in the studied devices with an established 2-D EMC transport model, details of which are given in [19], which has been validated

against many similar experimentally realized devices [2], [3]. As in [14], a doping notch next to the cathode contact was used to simulate the effect of the cathode contact to precipitate domain formation. A typical mesh of  $100 \times 100$  was used with up to 500 000 super-particles. Each super-particle represents a number of real particles such that the charge carried by the super-particles will reproduce the correct charge density, which is then used to calculate the electric field in each field adjusting time step. These particles are propagated classically between collisions according to their velocity, effective mass, and the prevailing electric field in the standard manner [20]. All electrons were weighted equally, and a typical run time was about 12 h to simulate 50 ps. A field adjusting time step of 1 fs was used, and the boundary conditions adopted were the usual Dirichlet conditions at the contacts with defined potentials and Neumann conditions at other boundaries assuming continuity of the electric field. For the dc calculations, an impressed voltage  $V_{DC}$  was applied at the contacts as the boundary conditions. A recognized drawback of Monte Carlo modeling is the statistical (noisy) nature of the simulated current. It is the feature that makes

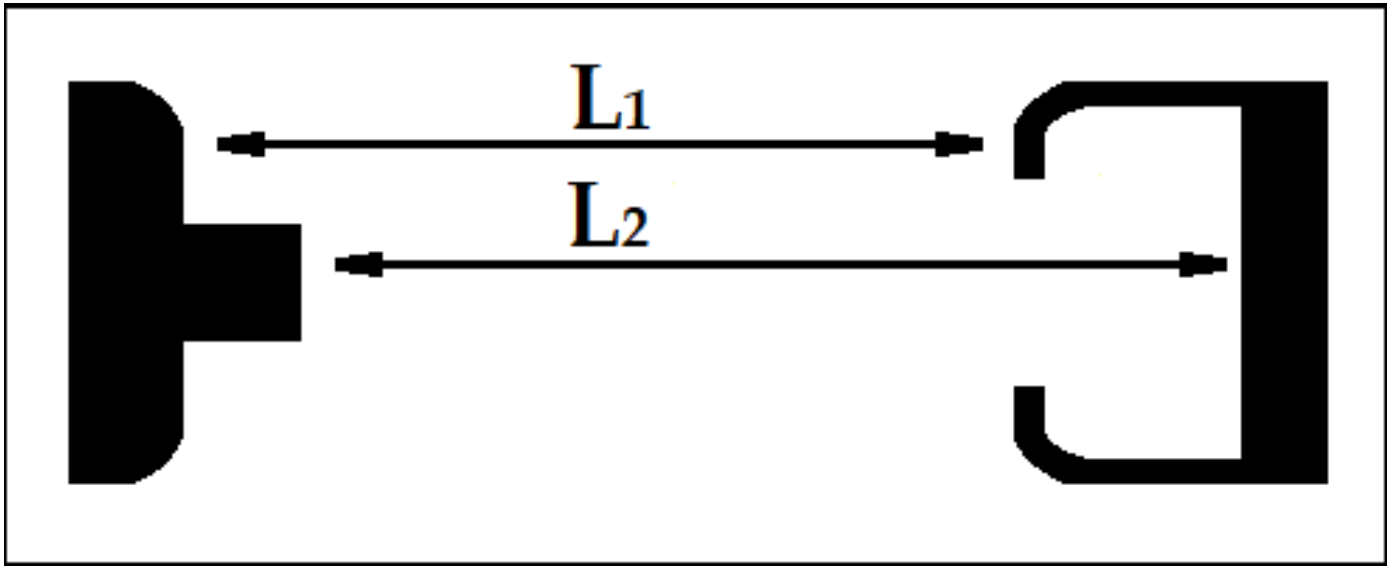


Fig. 1. Schematic of the novel planar Gunn diodes used here in the simulations.

linking a Monte Carlo model with an external circuit model difficult [21]. For devices in a resonant circuit, the interaction of the device and the circuit is described by assuming that steady-state oscillations have been established and the diode is driven by a known RF voltage  $V_{RF}$  such that  $V = V_{DC} + V_{RF} \sin(\omega t)$  in the standard manner [21]–[24]. To improve the statistics in this study, the current  $I(t)$  through the device was evaluated by averaging the charge output through each contact

(the number of super-particles passing through the contact together with displacement current) at each field adjusting time step over 40 output values, which equates to less than 0.1 ps. This is much less than the time period of the oscillations for the frequencies of interest (up to 350 GHz corresponding to a time period of 2.8 ps). We simulated a whole planar Gunn diode with a 24  $\mu\text{m}$  of channel length. A schematic of the simulated structure is shown in Fig. 1, and the process of arriving at this design will be discussed in Section III-A. Devices with channel widths  $L_1$  ranging from 1.30 to 1.60  $\mu\text{m}$  and  $L_2$  ranging from 1.44 to 1.46  $\mu\text{m}$  were investigated. As in [11], the simulations were done on the presumption of a lattice temperature of 300 K (room temperature).

Results will be presented for both transit-time- and delayed- mode oscillations. In the transit mode, the device is biased with a constant applied potential. For delayed-mode oscillations, there is a substantial ac feedback component (1 V) on a 2-V dc component so that the potential after each transit drops below the threshold for domain formation. A new domain will reform at the anode as the potential increases above the threshold again.

### III. ANALYSIS AND DISCUSSION OF RESULTS

#### A. Preliminary Investigation of Contact Shaping

Before discussing the results of the designed device, it is important to explain how the design was arrived at. Fig. 2 shows a schematic of the evolution of the design starting with a simple crenelated geometry [Fig. 2(a)]. The descriptive terminology is defined as follows: in a crenellation, the merlons are the “fingers” that extend toward the other electrode, and the gaps between the fingers are the crenels [see Fig. 2(a)]. In this design, it was found that a domain traveling from the cathode will first be incident on the leading edge of the anode, or merlon. As the domain advances into the crenel, it wraps around the merlon until finally it hits the bottom recess of the crenel. Because of the domain wrapping around the merlon, the current increase was found to be smooth and continuous, rather than delivering two distinct peaks of current corresponding to hitting the leading edge of the merlon and then the bottom recess of the crenel. In order to reduce the wrapping effect, attempts were made to shape the merlon in the form of a dovetail [Fig. 2(b)] which did improve the operation

of the device, and increased improvements were achieved by further hollowing out the merlon [Fig. 2(c)]. The smallest feature size on the anode is about 100 nm, which is experimentally realizable, and this will be discussed in Section III-D.

Returning to the simple crenelated design, as the domains hit the merlon, partial domains reform at the cathode opposite the merlons. Only when the rest of the domain passed through the bottom of the crenel do the corresponding parts of the domain reform at the cathode, by which time, the merlon parts of the domain have already made some progress on their transit. In this way, the newly formed domain is considerably distorted, and this distortion grows with each subsequent transit, eventually leading to chaotic current output. The merlon and crenel parts of the diode have different channel widths, and the domain structure and output current consequently become very complicated and out of phase with each other.

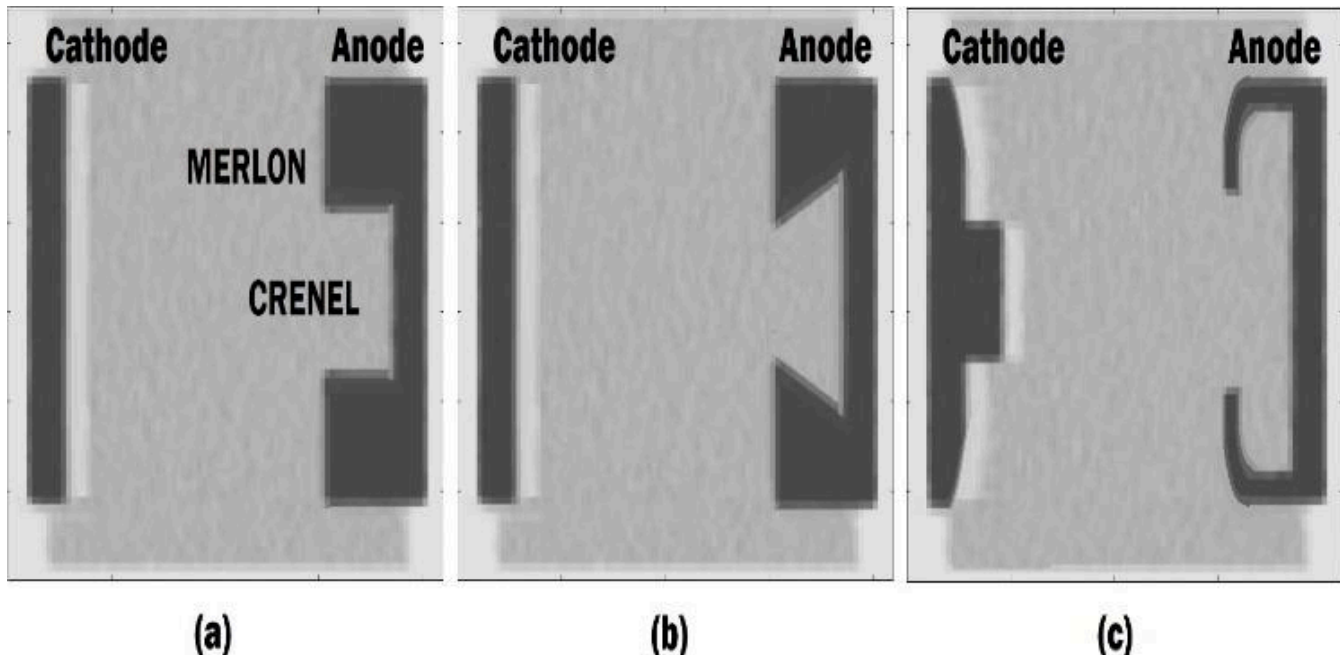


Fig. 2. (a) Schematic of the crenelated design anode contact.

(b) Schematic of the dovetail shape anode contact. (c) Schematic of the novel contacts planar Gunn diodes analyzed in this article.

The obvious solution to this is to operate the device in a delayed mode. In this mode, the feedback potential is such as to allow the potential to fall below the threshold value for domain formation, thus extinguishing any incipient domain at the anode. When the voltage once again increases above the threshold, a new fresh domain can reform, which will not suffer from any memory of previous transits.

This mode of operation will be discussed in Section III-C.

Another means by which different period problems can be mitigated is by using the negative differential resistivity of the electron transport. The shorter distance between the anode and cathode of the merlon part of the device leads to a higher field and a more slowly moving domain. The greater distance between anode and cathode in the crenel portion has a lower electric field and consequently faster domain; by careful selection of the applied bias and the distances between anode and cathode, a point of stationary transit time can be found where despite small differences in distance, the transit period is the same and so the different parts of the device can maintain a stationary phase difference with each other. Normal Gunn diodes will operate from their threshold to when breakdown occurs, which will give a voltage range of about 4 V, (depending on their size).

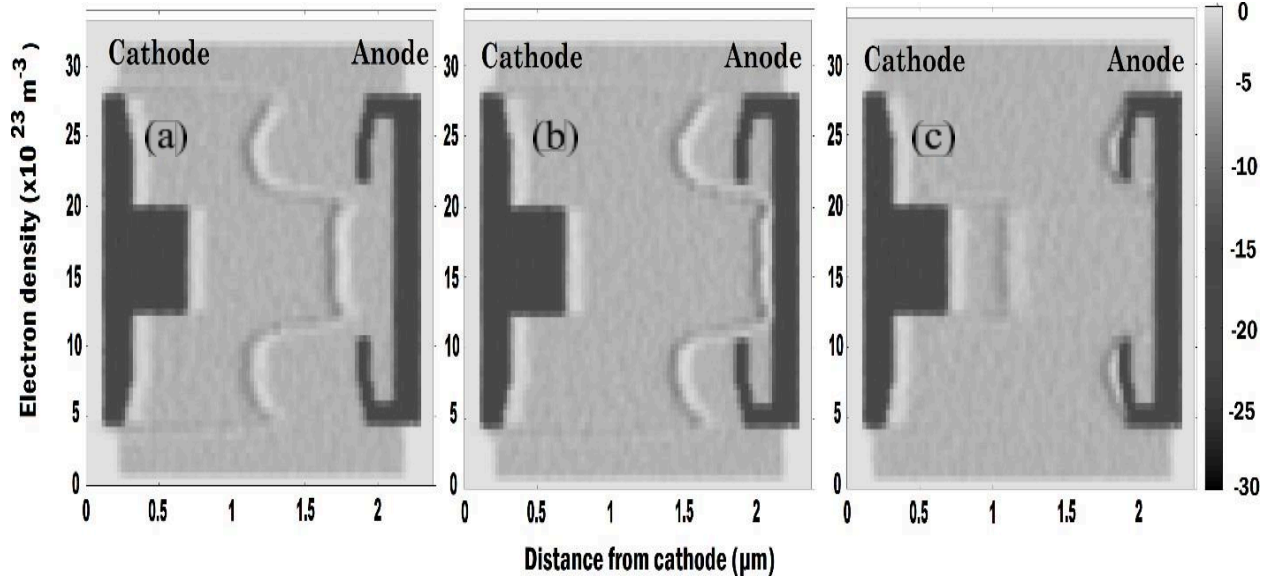


Fig. 3. (a)–(c) Electron density in a 22-μm-long device under the effect of 2.0-V bias at several instants during the transit region. (a) Domain forms at 55 ps from the cathode. (b) Same device 3.6 ps later, the domain has progressed further toward the anode. (c) After another 3.6 ps, the domain has progressed further toward and hit the edge anode. Parameters according to Fig. 1:  $L_1 = 1.60$  and  $L_2 = 1.46$  μm.

However, the requirement for stationary transit time reduces this range to about 0.5 V. Here, we found that the range of operating voltages was between

1.8 and 2.3 V with an optimal voltage of 2 V. We also found that including a merlon on the cathode,

opposite the crenel on the anode, to decrease the distance between anode and cathode in the crenel part of the device, was necessary to create a stable, periodic domain transit. The device was found to function for a range of values between 5.2 and 13.5  $\mu\text{m}$  to 8.5 and 7  $\mu\text{m}$  for a single anode merlon length to crenel length.

The optimal ratio was found to be 6.6–10.7  $\mu\text{m}$ , as shown in Fig. 3. Note that the relative transit lengths in this design are now reversed over the original simple crenelated design. Here, the cathode–anode merlon distance is now longer than the cathode–anode crenel distance. In this article, the lengths L1 and L2 (Fig. 1) were varied in the range discussed in Section II until the stationary point was found.

Finally, as in [11], it was found that the domains were vulnerable to attraction to any sharp corners on the contacts and this led to undesirable distortion of the domain. Blunting these corners as in [11] reduces this effect and further improved domain behavior.

### *B. Transit Time Mode*

Fig. 3 shows the domain structure in the diode after four transits of the domain after about 50 ps from the start of the simulation (to allow the device to settle down to steady periodic motion after the initial start-up) under a 2-V bias. It can be seen in Fig. 3(a) that at 53.2 ps, the domain has taken on the shape of the cathode. At 3.6 ps later, Fig. 3(b) shows the domain about to make contact with the crenel part of the anode, and the current in Fig. 4 can be seen to be increasing. begins to contact the merlon and the current consequently increases for the second peak [Fig. 3(c)]. Meanwhile, the new domain has already formed at the cathode merlon and is in transit while the new domain components are forming in the crenel regions of the anode (opposite the merlon regions of the anode). These two parts of the domain will then merge to become one domain again, as shown in Fig. 3(a).



The domain passes through the crenel and the current falls until at 60 ps when the domain

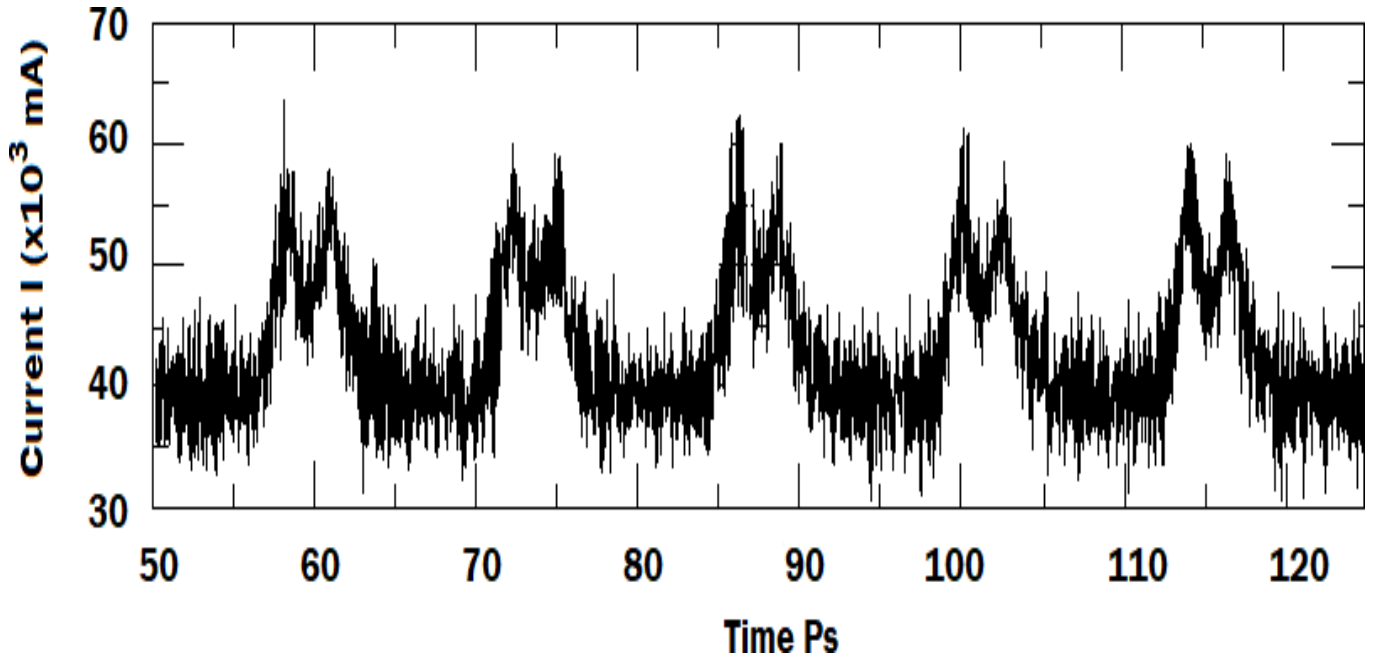


Fig. 4. Total current from Monte Carlo simulation of the transit time mode

Fig. 4 shows the current output from the device with the steady repeating oscillations with a period of 14 ps (70 GHz). The fine structure in the peaks corresponding to the domain being the first incident on the crenel, and then, the merlon has a period of 2.8 ps (350 GHz), five times greater than the natural period of the transit region length. Potentially, the device could be mounted in a high-Q circuit and tuned to extract the harmonic (in the above example, the fifth harmonic). The output current at the harmonic frequency for these devices will be higher than the output current for a conventional planar Gunn diode, thus offering the potential of THz operation with enhanced output power.

#### *C. Delayed-Domain Mode*

For the delayed-mode simulations, the optimum structure was found to be  $L_1 \pm 1.30$  and  $L_2 \pm 1.44$   $\mu\text{m}$ . An applied potential with a constant dc component of 2 V with a frequency-dependent amplitude of 1 V at a frequency of 45 GHz was found to work well in providing sufficient time to allow the domain to pass through the anode and sufficient change of potential to quench the new domain forming at the anode, thus enabling a fresh domain to reform at the cathode as the

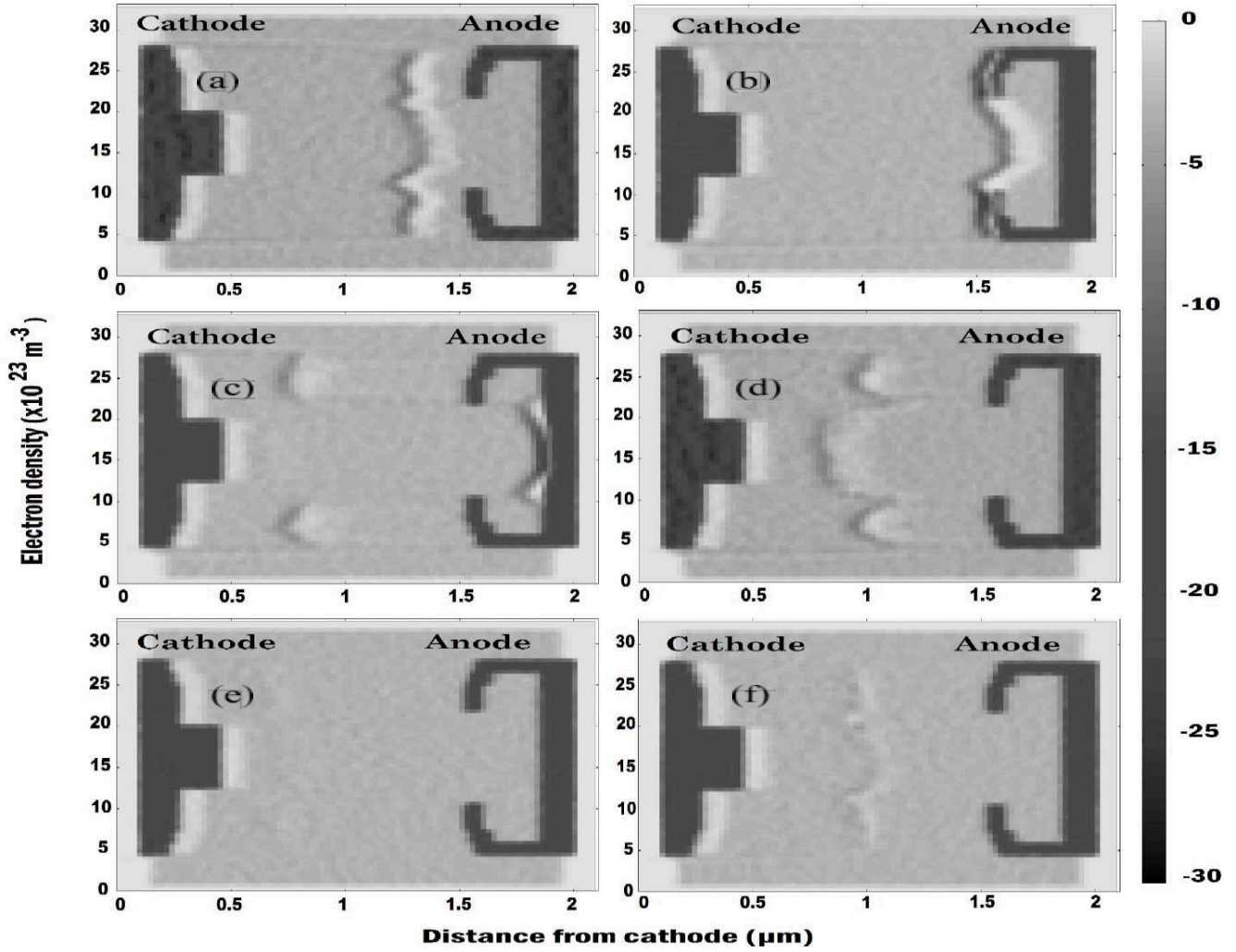


Fig. 5. (a)–(f) Electron density under the effect of 2.0-V bias at several instants during the transit region. (a) Domain forms at 47.1 ps from the cathode. (b) Same device 3.6 ps later, the domain contacts the merlons. (c) After another 3.6 ps, the domain contacts the crenel. (d) New distorted domain forms at 56.8 ps. (e) Domain is extinguished due to the falling voltage at 62.8 ps. (f) Domain reforms at 65.2 ps. Parameters according to Fig. 1:  $L_1 = 1.30$  and  $L_2 = 1.44 \mu\text{m}$ .

voltage will again increase above the threshold voltage. The simulated electron densities during the transit of the Gunn domain in this mode at 47, 50.7, 54.3, 56.8, 62.8, and 65.2 ps are shown in Fig. 5(a)–(f), respectively.

In Fig. 5(a), the domain can be seen traveling toward the anode, slightly distorted in places corresponding to the shape of the anode, but on the whole, quite straight. This moment corresponds to the trough in current at 47 ps in Fig. 6. In Fig. 5(b), the domain can be seen

to come into contact with the anode merlons, and this corresponds to the first peak in the current at 51 ps. For the following 2 ps, the current falls as the remaining domain travels toward the crenel part of the anode. Upon contact with the crenel at 54 ps [Fig. 5(c)], the current rises again. Note that the merlon component of the domain has already reformed at the cathode and is in transit.

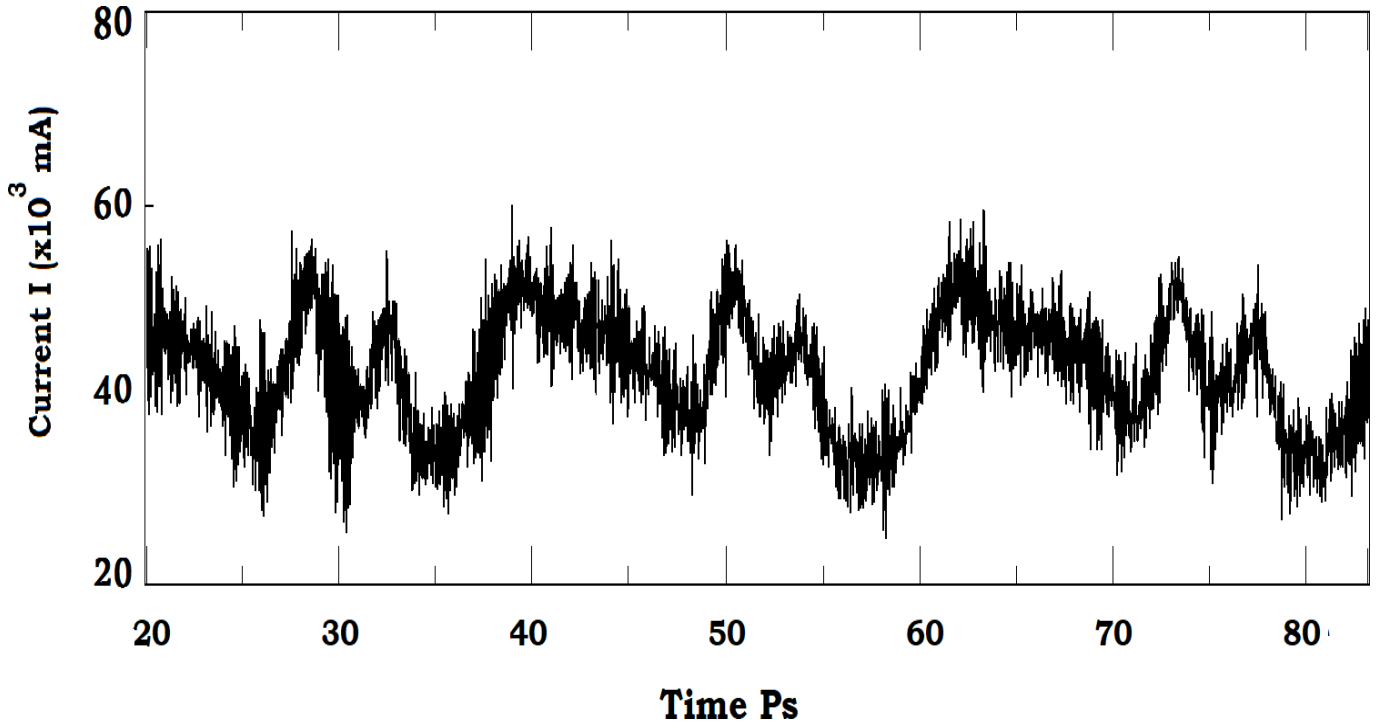


Fig. 6. Total current from Monte Carlo simulation of the delayed-domain mode.

Fig. 5(d) shows the complicated shape of the domain as the merlon and the crenel components have now reformed. If these transits were allowed to continue, the distortions on each subsequent transit would become greater and the output current waveform progressively more chaotic. However, at this point, the applied potential is about to fall below the threshold voltage for domain formation and the domain is extinguished, as shown in Fig. 5(e). Finally, when the voltage increases once again, the current increases (62 ps in Fig. 6) and a fresh and relatively straight domain reforms and can be seen in transit within the channel in Fig. 5(f) at 65 ps.

As can be seen in Fig. 6, the current waveform shows a lot of fine structure. The prominent peaks at 40 and 63 ps correspond to the 45-GHz delayed-mode potential and the reforming of the domains. The double peaks at 30, 52, and 75 ps are each 4 ps apart representing the contact of the domain with merlon and then the crenel. This represents a frequency component of 250 GHz.

#### *D. Proposed Fabrication Technology*

The current semiconductor device fabrication technology is capable of very small feature sizes down to few nm or smaller, but some III–V devices such as field-effect transistor (FET) and likewise planar Gunn diodes require dimensions longer than several micrometer for the width but with submicrometer sized channel gaps. Writing narrow channel gaps between long and wide contacts is difficult by electron beam lithography despite the small beam diameter due to electron beam proximity effects. This is one reason most FET devices with submicrometer gate lengths are achieved using the gate shadow to deposit the drain and source contact on either side of T-shaped gate. One other possibility could be deposit the gold and then etch small gaps, but it is relatively difficult to etch high-resolution gold patterns, and because of this, small gaps between metal contacts are difficult to fabricate using the conventional subtractive processing flow of metal deposition followed by resist patterning and metal etch. Thoms and Macintyre [25] previously showed that 100-nm gaps between 100- $\mu\text{m}$  square metal contacts can be realized using a trilayer of polydimethylglutarimide (PMGI) silicon nitride and UVIII resist. The UVIII resist layer is patterned by electron beam lithography. Reactive ion etching (RIE) is used to etch through the silicon nitride layer, and a low bias oxygen RIE process is used to etch the sacrificial PMGI layer. The silicon nitride layer is not etched by the plasma and so enables the PMGI layer to be etched back by a controlled amount to give profiles optimal for metal liftoff. We have demonstrated the fabrication of planar Gunn diodes using this technique [25]–[28] down to 100-nm channel gaps though we were only able to achieve 600-nm channel gap planar Gunn diodes which oscillated. Therefore, we have demonstrable techniques using a combination of several processes to achieve 100-nm channels, which will offer the possibility of a low cost and fully integrated THz source.

#### **IV. CONCLUSION**

We have shown it is theoretically possible and experimentally realizable, using shaped anodes and cathodes in a planar Gunn diode to produce stable periodic Gunn domain transits, which will yield current waveforms with a fine frequency structure considerably higher in frequency than the nominal transit time of the domain across the channel.

Any shaping of either anode or cathode electrodes can allow distorted domains to develop, with effectively different periods dependent on the travel time between the two shaped contacts making the channel. This distortion can lead to extremely complicated and even chaotic output current waveforms. However, by careful choice of the widths of the channel, it is possible to achieve stable operation by two methods: by utilizing the property of negative differential resistivity to find points of stationary time of transit, despite small differences in transit region length and by using delayed-mode oscillations in which the Gunn domains are quenched after each transit forming anew with no memory of previous transits.

As mentioned in the Introduction, so far, the RF output power and efficiency of the standard planar Gunn diode with the straight-edged anode and cathode electrodes have been disappointing. Therefore, the prospects for a reasonable amount of power extraction in a fifth harmonic might at first sight not look very good with the existing research devices produced so far. However, theoretical calculations have shown that the output power and efficiency should be at least comparable to the vertical Gunn diodes, and a recent theoretical work [11] has shown that by improving the planar Gunn diode electrode geometry, enhanced domain propagation can be obtained, thus leading to the potential of substantial improvements in both RF output power and efficiency. In addition, the planar Gunn diode concept has the potential to be fully integrated into MMIC technology and offers the prospect of adding multiple devices to improve power and efficiency. Normally, in Gunn diode systems, only the second or third harmonic is chosen as a practical power source since higher harmonics will produce an almost unusable RF output power. However, this work indicates that these devices are actually generating current output at this harmonic and this suggests that the potential for useful power generation is a real possibility in chip-based terahertz systems that would be mass producible. The power efficiency may still remain low, but with multiple integrated devices, a reasonable power generation is a real prospect. It is also interesting to note that the ability to shape waveforms by sculpturing the anode and cathode may have other interesting waveform-shaping applications.

## ACKNOWLEDGMENT

The authors would like to thank the University of Aberdeen, Aberdeen, U.K., for providing the necessary support.

## REFERENCES

- [1] P. J. Bulman, G. S. Hobson, and B. C. Taylor, *Transferred Electron Devices*. New York, NY, USA: Academic, 1972.
- [2] A. Khalid *et al.*, "A planar gunn diode operating above 100 GHz," *IEEE Electron Device Lett.*, vol. 28, no. 10, pp. 849–851, Oct. 2007, doi: 10.1109/LED.2007.904218.
- [3] A. Khalid *et al.*, "Terahertz oscillations in an  $\text{In}_{0.53}\text{Ga}_{0.47}\text{As}$  submicron planar Gunn diode," *J. Appl. Phys.*, vol. 115, no. 11, Mar. 2014, Art. no. 114502.
- [4] V. Gruzinskis *et al.*, "Gunn effect in n-InP MOSFET at positive gate bias and impact ionization conditions," in *Proc. Int. Workshop Comput. Electron. (IWCE)*, Jun. 2014, pp. 1–2.
- [5] S. García, I. Íñiguez-de-la-Torre, S. Pérez, J. Mateos, and T. González, "Numerical study of sub-millimeter Gunn oscillations in InP and GaN vertical diodes: Dependence on bias, doping, and length," *J. Appl. Phys.*, vol. 114, no. 7, Aug. 2013, Art. no. 074503.
- [6] S. Pérez, T. González, D. Pardo, and J. Mateos, "Terahertz gunn-like oscillations in InGaAs/InAlAs planar diodes," *J. Appl. Phys.*, vol. 103, no. 9, May 2008, Art. no. 094516, doi: 10.1063/1.2917246.
- [7] M. I. Maricar, "Design of circuits to enhances the performace of high frequency planar Gunn diodes," Ph.D. dissertation, Fac. Technol., De Montfort Univ., Leicester, U.K., 2014. [Online]. Available: <http://hdl.handle.net/2086/10858>
- [8] J. Glover *et al.*, "Thermal profiles within the channel of planar Gunn diodes using micro-particle sensors," *IEEE Electron Device Lett.*, vol. 38, no. 9, pp. 1325–1327, Sep. 2017, doi: 10.1109/LED.2017.2731961.
- [9] M. Montes Bajo *et al.*, "Impact ionisation electroluminescence in planar GaAs-based heterostructure Gunn diodes: Spatial distribution and impact of doping non-uniformities," *J. Appl. Phys.*, vol. 113, no. 12, Mar. 2013, Art. no. 124505, doi: 10.1063/1.4798270.
- [10] M. Montes *et al.*, "Reduction of impact ionization in GaAs- based planar Gunn diodes by anode contact design," *IEEE Trans. Electron Devices*, vol. 59, no. 3, pp. 654–660, Mar. 2012, doi: 10.1109/TED.2011.2177094.
- [11] A. Mindil, G. M. Dunn, A. Khalid, and C. H. Oxley, "Investigation of contact edge effects in the channel of planar Gunn diodes," *IEEE Trans. Electron Devices*, vol. 67, no. 1, pp. 53–56, Jan. 2020, doi: 10.1109/TED.2019.2951301.
- [12] L. L. Bonilla, R. Escobedo, and F. Higuera, "Axisymmetric pulse recycling and motion in bulk semiconductors," *J. Phys. Rev. E*, vol. 65, Dec. 2001, Art. no. 016607.
- [13] M. Shoji, "Functional bulk semiconductor oscillators," *IEEE Trans. Electron Devices*, vol. ED-14, no. 9, pp. 535–546, Sep. 1967.
- [14] N. J. Pilgrim, A. Khalid, C. Li, G. M. Dunn, and D. R. S. Cumming, "Contact shaping in planar Gunn diodes," *Phys. Status Solidi (C)*, vol. 8, no. 2, pp. 313–315, Feb. 2011, doi: 10.1002/pssc.201000539.
- [15] M. Shur, *GaAs Devices and Circuits*. New York, NY, USA: Plenum, 1987.
- [16] B. Li, H. Liu, Y. Alimi, and A. Song, "Simulation investigation of multiple domain observed in  $\text{In}_{0.23}\text{Ga}_{0.77}\text{As}$  planar Gunn diode," *Int. J. Hydrogen Energy*, vol. 41, no. 35, pp. 15772–15776, Sep. 2016, doi: 10.1016/j.ijhydene.2016.04.055.
- [17] S. Montanari, "Fabrication and characterization of planar Gunn diodes for monolithic microwave integrated circuits," Forschungszentrum Jülich, Jülich, Germany, Tech. Rep., 2005.
- [18] F. Amir, "Advanced physical modelling of step graded Gunn diode for high power TeraHertz sources," Ph.D. dissertation, Fac. Eng. Phys. Sci., Univ. Manchester, Manchester, U.K., 2011. [Online]. Available: <https://core.ac.uk/download/pdf/40021111.pdf>
- [19] N. J. Pilgrim, A. Khalid, G. M. Dunn, and D. R. S. Cumming, "Gunn oscillations in planar heterostructure diodes," *Semicond. Sci. Technol.*, vol. 23, May 2008, Art. no. 075013.
- [20] M. V. Fischetti, "Monte Carlo simulation of transport in technologically significant semiconductors of the diamond and zinc-blende structures.  
1. Homogeneous transport," *IEEE Trans. Electron Devices*, vol. 38, no. 3, pp. 634–649, Mar. 1991.
- [21] R. Kamoua, "Monte Carlo-based harmonic balance technique for the simulation of high-frequency TED oscillators," *IEEE Trans. Microw. Theory Techn.*, vol. 46, no. 10, pp. 1376–1381, Oct. 1998.

- [22] R. Kamoua, H. Eisele, and G. I. Haddad, "D-band (110–170 GHz) InP gunn devices," *Solid-State Electron.*, vol. 36, no. 11, pp. 1547–1555, Nov. 1993.
- [23] R. Judaschke, "Comparison of modulated impurity-concentration InP transferred electron devices for power generation at frequencies above 130 GHz," *IEEE Trans. Microw. Theory Techn.*, vol. 48, no. 4, pp. 719–724, Apr. 2000.
- [24] M. F. Zybura, S. H. Jones, G. Tait, and J. M. Duva, "Efficient computer aided design of GaAs and InP millimeter wave transferred electron devices including detailed thermal analysis," *Solid-State Electron.*, vol. 38, no. 4, pp. 873–880, Apr. 1995.
- [25] S. Thoms and D. S. Macintyre, "Long nanoscale gaps on III–V substrates by electron beam lithography," *J. Vac. Sci. Technol. B, Microelectron.*, vol. 30, no. 6, Nov. 2012, Art. no. 06F305.
- [26] A. Khalid, S. Thoms, D. Macintyre, I. G. Thayne, and D. R. S. Cumming, "Fabrication of submicron planar Gunn diode," in *Proc. 26th Int. Conf. Indium Phosph. Rel. Mater.*, Montpellier, France, May 2014, pp. 11–15, doi: 10.1109/ICIPRM.2014.6880542.
- [27] A. Khalid, C. Li, V. Papageorgiou, N. J. Pilgrim, G. M. Dunn, and D. R. S. Cumming, "A 218-GHz second-harmonic multiquantum well GaAs-based planar Gunn diodes," *Microw. Opt. Technol. Lett.*, vol. 55, no. 3, pp. 686–688, Mar. 2013, doi: 10.1002/mop. 27393.
- [28] A. Khalid *et al.*, "In<sub>0.53</sub>Ga<sub>0.47</sub>As planar Gunn diodes operating at a fundamental frequency of 164 GHz," *IEEE Electron Device Lett.*, vol. 34, no. 1, pp. 39–41, Jan. 2013, doi: 10.1109/LED.2012.2224841.